LETTERS

Intronic microRNA precursors that bypass Drosha processing

J. Graham Ruby[1,2]*, Calvin H. Jan[1,2]* & David P. Bartel[1,2]

MicroRNAs (miRNAs) are ~22-nucleotide endogenous RNAs that often repress the expression of complementary messenger RNAs[1]. In animals, miRNAs derive from characteristic hairpins in primary transcripts through two sequential RNase III-mediated cleavages; Drosha cleaves near the base of the stem to liberate a ~60-nucleotide pre-miRNA hairpin, then Dicer cleaves near the loop to generate a miRNA:miRNA* duplex[2,3]. From that duplex, the mature miRNA is incorporated into the silencing complex. Here we identify an alternative pathway for miRNA biogenesis, in which certain debranched introns mimic the structural features of pre-miRNAs to enter the miRNA-processing pathway without Drosha-mediated cleavage. We call these pre-miRNAs/introns 'mirtrons', and have identified 14 mirtrons in *Drosophila melanogaster* and another four in *Caenorhabditis elegans* (including the reclassification of *mir-62*). Some of these have been selectively maintained during evolution with patterns of sequence conservation suggesting important regulatory functions in the animal. The abundance of introns comparable in size to pre-miRNAs appears to have created a context favourable for the emergence of mirtrons in flies and nematodes. This suggests that other lineages with many similarly sized introns probably also have mirtrons, and that the mirtron pathway could have provided an early avenue for the emergence of miRNAs before the advent of Drosha.

While examining sequencing data of small RNAs from *D. melanogaster*[4], we observed clusters of small RNAs originating from the outer edges of an annotated 56-nucleotide (56-nt) intron (Fig. 1a). These sets of reads (each read representing an independently sequenced complementary DNA) had properties similar to those observed previously for miRNA:miRNA* duplexes[5], in that each set had a more consistent 5′ than 3′ terminus, and the two sets were complementary to each other, with the dominantly abundant species of each set forming 2-nt 3′ overhangs when paired to each other. Moreover, the sequence and predicted secondary structure of the intron were conserved in a pattern resembling that of pre-miRNAs[6] (Fig. 1b, c). We annotated this locus as *mir-1003*.

Despite these clearly miRNA-like properties, semblance to canonical miRNA primary transcripts (pri-miRNAs) stopped abruptly at the borders of the intron. Pairing at the base of the hairpin did not extend beyond the miRNA:miRNA* duplex—that is, beyond the splice sites. In place of extended pairing, which is needed for pri-miRNA cleavage by Drosha (ref. 7), the intron had conserved canonical splice sites (Fig. 1b), leading to the model that this miRNA did not arise from a canonical miRNA biogenesis pathway but instead arose from an alternative pathway in which splicing, rather than Drosha, defined the pre-miRNA (Fig. 1d). Consistent with this model, spliced lariats linearized by the lariat debranching enzyme bear 5′ monophosphates[8] and 3′ hydroxyls[9], the same moieties found in pre-miRNAs[1,3,10].

Thirteen additional pre-miRNAs/introns, termed mirtrons, were found in a search of other loci with similar properties (*mir-1004–1016*, Supplementary Table S1). The most abundant RNA species from each of the 14 mirtrons, annotated as the mature miRNA, derived from the 3′ arm of its hairpin. Such bias was consistent with the known 5′ nucleotide biases of miRNAs, which frequently begin with a U and rarely with a G (ref. 11). The near-ubiquitous intronic 5′ G, together with other requirements at intron 5′ ends[12], would place unfavourable constraints on miRNAs deriving from the 5′ arm of a mirtron, whereas the species from the 3′ arm would have more freedom. As expected, the species from the 3′ arms, like canonical miRNAs, usually had a 5′ U (12/14 mirtrons).
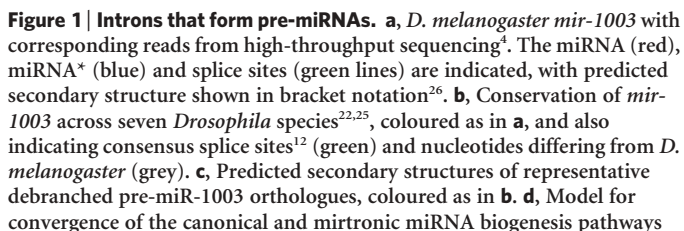
To test whether the small RNAs from mirtrons were functional miRNAs or inactive degradation intermediates, we assessed the gene-silencing capacities of miR-1003 and miR-1006 in *Drosophila* S2 cells. In animals, extensive complementarity leads to cleavage of the target mRNA, but post-transcriptional repression is more commonly mediated by less extensive complementarity, primarily involving pairing to a 5′ region of the miRNA known as the miRNA seed[1]. miR-1003 and miR-1006 repressed reporter genes with perfectly complementary sites, with the repression levels approaching that observed for the *let-7* miRNA and an analogous reporter (Fig. 1e). In addition, both mirtronic miRNAs repressed reporter genes containing *Drosophila* untranslated region (UTR) fragments with seed-based matches typical of metazoan miRNA targets. Conservation of the miR-1003 and miR-1006 seeds (Fig. 1d, Supplementary Table S1) suggested an *in vivo* role for such mirtron-mediated repression; target predictions for conserved mirtronic miRNAs are provided (http://www.targetscan.org).

Having established that mirtrons can direct miRNA-like gene repression, we tested the dependence of mirtron processing on splicing and debranching. A mutant *mir-1003* with a substitution that impaired splicing (3′ Mut) generated little pre- or mature miR-1003 (Fig. 2a, b) and displayed significantly less silencing activity (Fig. 1e). Mutations disrupting the 5′ splice site (5′ Mut) also impaired splicing and miR-1003 accumulation (Fig. 2a, b). Coexpressing a mutant U1 small nuclear RNA (snRNA; U1-3G) that had compensatory changes designed to restore splice site recognition[13] restored splicing of *mir-1003* 5′ Mut (Fig. 2b). Rescuing splicing also restored the levels of pre- and mature miR-1003 (Fig. 2b). These results demonstrated that splicing was required for mirtron maturation and function, which contrasts with the splicing-independent biogenesis of canonical miRNAs found within introns[14].

We next used RNA interference (RNAi) knockdown experiments to examine the trans-factor requirements for miR-1003 and miR-1006 biogenesis in *Drosophila* cells. As predicted by our model, in which mirtrons enter the miRNA biogenesis pathway after splicing and debranching, targeting the mRNA of lariat debranching enzyme

[1]Whitehead Institute for Biomedical Research, 9 Cambridge Center, Cambridge, Massachusetts 02142, USA. [2]Howard Hughes Medical Institute and Department of Biology, Massachusetts Institute of Technology, Cambridge, Massachusetts 02139, USA.
*These authors contributed equally to this work.

Figure 1 | Introns that form pre-miRNAs. a, *D. melanogaster mir-1003* with corresponding reads from high-throughput sequencing[4]. The miRNA (red), miRNA* (blue) and splice sites (green lines) are indicated, with predicted secondary structure shown in bracket notation[26]. **b**, Conservation of *mir-1003* across seven *Drosophila* species[22,25], coloured as in **a**, and also indicating consensus splice sites[12] (green) and nucleotides differing from *D. melanogaster* (grey). **c**, Predicted secondary structures of representative debranched pre-miR-1003 orthologues, coloured as in **b**. **d**, Model for convergence of the canonical and mirtronic miRNA biogenesis pathways (see text). **e**, MicroRNA regulation of luciferase reporters in S2 cells. Plotted is the ratio of repression for wild-type versus mutated sites, normalized to that with the indicated non-cognate miRNA. Bar colour represents the cotransfected miRNA expression plasmid; coloured lines below indicate the cognate miRNA for the specified reporter. Error bars represent the third largest and smallest values from 12 replicates (four independent experiments, each with three transfections; *$P < 0.01$, **$P < 0.0001$, Wilcoxon rank-sum test).

reduced the amount of pre- and mature mirtronic miRNAs without impeding canonical miRNA maturation (Fig. 2c, d). For each mirtron, a probe to the 5′ end of the intron (probe 1) detected both the pre-miRNA hairpin and the accumulating lariat, whereas a probe to the 3′ end of the intron (probe 2) detected the pre-miRNA but failed to detect the lariat, presumably owing to overlap with the branch-point (Supplementary Fig. S1a). Altered relative mobility on gels with different polyacrylamide densities confirmed detection of the

Figure 2 | Mirtrons are spliced as introns and diced as pre-miRNAs. a, Schematic of splice-site mutations. **b**, Base pairing between the indicated U1a and *mir-1003* RNAs (left), and RT–PCR and northern-blot analyses of *mir-1003* variants from **a**. The miR-1003 bands in lane 2 were attributed to endogenous miRNA. **c**, Northern blots analysing *let-7* and *mir-1003* maturation in cells treated with double-stranded RNAs (dsRNAs) corresponding to indicated genes. Shown are results from one membrane,

sequentially stripped and probed for *let-7* RNA, pre-miR-1003/lariat (probe 1), pre-miR-1003/miR-1003 (probe 2), and U6. Previously validated dsRNAs were used[28,29], except for lariat debranching enzyme (CG7942, which we name *ldbr*), for which two unique dsRNAs were used. Knockdowns were confirmed by monitoring mRNA level and protein function (Supplementary Fig. S2). Quantification of band intensities is provided (Supplementary Table S3). *Lariat. **d**, Analysis of *mir-1006* processing, as in **c**.

mirtron lariat (Supplementary Fig. S1b). The debranching knockdown results, together with those of the splice-site mutations and rescue, demonstrated that the intron lariat was an intermediate on the pathway of mirtronic miRNA biogenesis.

Knockdown of other miRNA biogenesis factors further supported our model. As expected if debranched mirtrons enter the later steps of the miRNA pathway rather than the short interfering RNA (siRNA) pathway[3], knockdown of *dicer-1* or its partner, *loquacious*, increased the ratio of pre- to mature mirtronic miRNA, whereas knockdown of *dicer-2* or its partner, *r2d2*, did not (Fig. 2c, d). Knockdown of *drosha* decreased pre- and mature *let-7* RNA accumulation, with little effect on mature miR-1003 or miR-1006 accumulation and a modest effect on mirtronic pre-miRNAs (Fig. 2c, d). The more modest effect on mirtronic pre- and mature miRNAs supported the idea that mirtronic pre-miRNAs are not Drosha cleavage products. The decrease of mirtronic pre-miRNA that was observed would be explained if Drosha bound mirtronic pre-miRNAs, stabilized them from degradation, and perhaps facilitated their loading into the nuclear export machinery. The decrease could also reflect increased Dicer-1 accessibility in the *drosha* knockdown due to reduced substrate competition from endogenous pre-miRNAs. In this case, simultaneous knockdown of *dicer-1* and *drosha* would lead to a more substantial accumulation of pre-miRNAs derived from mirtrons than from canonical miRNAs, as was observed for pre-miR-1003 and pre-miR-1006 compared to *let-7* pre-miRNA (Fig. 2c, d).

The distribution of intron lengths, which varies widely in different organims[12,15], would influence the probability of new mirtrons arising during evolution. The introns of *Drosophila* share a similar length distribution with the annotated pre-miRNAs, producing a context particularly well suited to the emergence to mirtrons (Fig. 3a, c). *C. elegans* also has a substantial number of pre-miRNA-sized introns. Indeed, examination of prior miRNA annotations revealed that *mir-62*, which produces a highly conserved nematode miRNA that was among the very first to be cloned in animals[11,16], had mirtron-like properties (Fig. 3b). Like the mirtrons of *D. melanogaster*, the base pairing capacity of the sequence surrounding pre-miR-62 ended at the border of the host intron, and the most abundant miRNA 3′ terminus corresponded to the 3′ splice site (with the single read whose 3′ terminus extended into the 3′ exon attributable

to untemplated nucleotide addition to the miRNA 3′ end[5]). A directed search of *C. elegans* small RNA sequences[5] revealed three more mirtrons, annotated here as *mir-1018–1020* (Supplementary Table S2).

Even if only a very small portion of debranched introns can form secondary structures resembling those of pre-miRNAs, the abundance of pre-miRNA-sized introns in flies and nematodes would allow a large absolute number of candidate mirtrons to emerge over evolutionary timescales. Whether they persist as functional mirtrons depends on the selective advantage conferred to the host organism as a consequence of their gene-repression activities. This model for mirtron emergence predicts that, at any historical point, some introns will be processed as mirtrons that provide no advantage to the organism but have yet to be eliminated by natural selection or neutral drift. Accordingly, some but not all processed *D. melanogaster* mirtrons were significantly more conserved in *Drosophila pseudoobscura* than were most small introns, and the same trend was observed for *C. elegans* mirtrons in *Caenorhabditis briggsae* (Fig. 3d). The three most conserved *D. melanogaster* mirtrons (*mir-1003/1006/1010*) gave rise to more reads than 27%, 16% and 4% of the non-mirtronic miRNAs conserved to *D. pseudoobscura*, respectively[4], while the most conserved *C. elegans* mirtron (*mir-62*) gave rise to more reads than 52% of the non-mirtronic miRNAs conserved to *C. briggsae*[5].

Compared to flies and nematodes, mammals have few pre-miRNA-sized introns[12,15] (Fig. 3a), perhaps explaining why we found no mirtrons among the annotated mammalian miRNAs[17]. Nonetheless, high-throughput sequencing of mammalian small RNAs might yet reveal mirtrons. In plants, miRNA processing could similarly bypass one of the RNase III cleavages, although plant mirtrons have not yet been identified[1,17]. Moreover, lineages with long introns might have other types of intronic miRNAs that bypass Drosha-mediated cleavage. This possibility was raised by *mir-1017*, whose putative pre-miRNA 5′ end, but not 3′end, matched the 5′ splice site of its host intron (Supplementary Table S1). In contrast to true mirtrons, miRNAs of this type would depend on a nuclease to cleave their extensive 3′overhangs, as observed for the U14 snRNA derived from an intron of *hsc70* (ref. 18). This mechanism, together with that of mirtron processing, would enable miRNAs to emerge in any organism with both splicing and post-transcriptional RNA silencing,

Figure 3 | Emergence and conservation of mirtrons in species with appropriately sized introns. a, Distributions of intron (orange) and pre-miRNA (green) lengths from the indicated species. Introns and pre-miRNAs were binned by length. **b**, Intron and associated reads of *C. elegans mir-62* (ref. 5), coloured as in Fig. 1a. Reads with untemplated nucleotides added at their 3′ terminus are shown below. **c**, Distributions of pre-miRNA (green) and mirtron (grey) lengths from *D. melanogaster* and *C. elegans*. **d**, Conservation of all 40–90-nt introns (orange) versus mirtrons (grey) from *D. melanogaster* (percentage identity shared with *D. pseudoobscura*) and *C. elegans* (percentage identity shared with *C. briggsae*).

even those lacking the specialized RNase III enzyme Drosha or its plant counterpart, DICER-LIKE1 (ref. 1). In this scenario, miRNAs might have emerged in ancient eukaryotes before the advent of modern miRNA biogenesis pathways.

METHODS SUMMARY

Computational methods. *D. melanogaster* small RNAs were from 2,075,098 high-throughput pyrosequencing reads[4] and are available at the GEO. *C. elegans* small RNA sequences were from ref. 5. Introns were as annotated in FlyBase (v4.2)[19], WormBase (release WS120)[20] and human RefSeq annotations[21] available through UCSC (hg17)[22]. Percentage conservation of *D. melanogaster*[23] and *D. pseudoobscura*[24] introns was calculated as the number of identity matches between the two orthologous introns in the multiZ alignment[22,25] divided by the length of the longer intron. *C. elegans* intron conservation was similarly determined using multiZ alignments[22] of the *C. elegans* and *C. briggsae* (WormBase cb25.agp8) genomes[20,22]. Pre-miRNA lengths were the sum of the miRNA length, the miRNA* length, and the length of intervening sequence, calculated after using RNAfold[26] to predict the structure of annotated miRNA hairpins (miRBase v9.1)[17] and inferring the miRNA* by assuming 2-nt 3′ overhangs when paired with the annotated miRNA.

Analysis of function and biogenesis. Mirtron minigenes containing flanking exons were amplified from genomic DNA and cloned into expression vectors, pMT-puro or p2032 (ref. 27). Similar plasmids were constructed for a 780-basepair (780-bp) fragment centred on the *let-7* hairpin. Luciferase reporters were constructed with 3′ UTRs (Supplementary Table S3) amplified from genomic DNA. U1 plasmids were constructed as described[13]. Mutations to seed sites (reporters) or splice sites (minigenes) were introduced by Quikchange site-directed mutagenesis (Stratagene). After RNAi knockdown[28,29], miRNA expression was induced with 500 μM CuSO$_4$, then 12 h post-induction RNA was extracted with TRI reagent and analysed on northern blots[5]. *Renilla* (reporter) and firefly (control) luciferase plasmids were cotransfected with miRNA-expressing plasmid into S2 cells. Fold repression was calculated by dividing normalized luciferase activity for mutant reporters by that of wild-type reporters in the presence of cognate miRNA. Transfection with non-cognate miRNA served as a specificity control.

Full Methods and any associated references are available in the online version of the paper at www.nature.com/nature.

1. Bartel, D. P. MicroRNAs: genomics, biogenesis, mechanism, and function. *Cell* **116**, 281–297 (2004).
2. Lee, Y. *et al.* The nuclear RNase III Drosha initiates microRNA processing. *Nature* **425**, 415–419 (2003).
3. Tomari, Y. & Zamore, P. D. Perspective: machines for RNAi. *Genes Dev.* **19**, 517–529 (2005).
4. Ruby, J. G. *et al.* Biogenesis, expression, and target predictions for an expanded set of microRNA genes in *Drosophila. Genome Res.* (in the press).
5. Ruby, J. G. *et al.* Large-scale sequencing reveals 21U-RNAs and additional microRNAs and endogenous siRNAs in *C. elegans. Cell* **127**, 1193–1207 (2006).
6. Lim, L. P. *et al.* The microRNAs of *Caenorhabditis elegans. Genes Dev.* **17**, 991–1008 (2003).
7. Han, J. *et al.* Molecular basis for the recognition of primary microRNAs by the Drosha-DGCR8 complex. *Cell* **125**, 887–901 (2006).
8. Ruskin, B. & Green, M. R. An RNA processing activity that debranches RNA lariats. *Science* **229**, 135–140 (1985).
9. Padgett, R. A., Konarska, M. M., Grabowski, P. J., Hardy, S. F. & Sharp, P. A. Lariat RNA's as intermediates and products in the splicing of messenger RNA precursors. *Science* **225**, 898–903 (1984).
10. Hutvagner, G. *et al.* A cellular function for the RNA-interference enzyme Dicer in the maturation of the *let-7* small temporal RNA. *Science* **293**, 834–838 (2001).
11. Lau, N. C., Lim, L. P., Weinstein, E. G. & Bartel, D. P. An abundant class of tiny RNAs with probable regulatory roles in *Caenorhabditis elegans. Science* **294**, 858–862 (2001).
12. Lim, L. P. & Burge, C. B. A computational analysis of sequence features involved in recognition of short introns. *Proc. Natl Acad. Sci. USA* **98**, 11193–11198 (2001).
13. Lo, P. C., Roy, D. & Mount, S. M. Suppressor U1 snRNAs in *Drosophila. Genetics* **138**, 365–378 (1994).
14. Kim, Y. K. & Kim, V. N. Processing of intronic microRNAs. *EMBO J.* **26**, 775–783 (2007).
15. Yandell, M. *et al.* Large-scale trends in the evolution of gene structures within 11 animal genomes. *PLoS Comput. Biol.* **2**, e15 (2006).
16. Lee, R. C. & Ambros, V. An extensive class of small RNAs in *Caenorhabditis elegans. Science* **294**, 862–864 (2001).
17. Griffiths-Jones, S. The microRNA registry. *Nucleic Acids Res.* **32**, D109–D111 (2004).
18. Leverette, R. D., Andrews, M. T. & Maxwell, E. S. Mouse U14 snRNA is a processed intron of the cognate hsc70 heat shock pre-messenger RNA. *Cell* **71**, 1215–1221 (1992).
19. Grumbling, G. & Strelets, V. FlyBase: anatomical data, images and queries. *Nucleic Acids Res.* **34**, D484–D488 (2006).
20. Stein, L., Sternberg, P., Durbin, R., Thierry-Mieg, J. & Spieth, J. WormBase: network access to the genome and biology of *Caenorhabditis elegans. Nucleic Acids Res.* **29**, 82–86 (2001).
21. Pruitt, K. D., Tatusova, T. & Maglott, D. R. NCBI Reference Sequence (RefSeq): a curated non-redundant sequence database of genomes, transcripts and proteins. *Nucleic Acids Res.* **33**, D501–D504 (2005).
22. Karolchik, D. *et al.* The UCSC genome browser database. *Nucleic Acids Res.* **31**, 51–54 (2003).
23. Adams, M. D. *et al.* The genome sequence of *Drosophila melanogaster. Science* **287**, 2185–2195 (2000).
24. Richards, S. *et al.* Comparative genome sequencing of *Drosophila pseudoobscura*: chromosomal, gene, and cis-element evolution. *Genome Res.* **15**, 1–18 (2005).
25. Blanchette, M. *et al.* Aligning multiple genomic sequences with the threaded blockset aligner. *Genome Res.* **14**, 708–715 (2004).
26. Hofacker, I. L. *et al.* Fast folding and comparison of RNA secondary structures. *Mh. Chem.* **125**, 167–188 (1994).
27. Brennecke, J., Stark, A., Russell, R. B. & Cohen, S. M. Principles of microRNA-target recognition. *PLoS Biol.* **3**, e85 (2005).
28. Dorner, S. *et al.* A genomewide screen for components of the RNAi pathway in *Drosophila* cultured cells. *Proc. Natl Acad. Sci. USA* **103**, 11880–11885 (2006).
29. Forstemann, K. *et al.* Normal microRNA maturation and germ-line stem cell maintenance requires Loquacious, a double-stranded RNA-binding domain protein. *PLoS Biol.* **3**, e236 (2005).
30. Lim, L. P. *et al.* Microarray analysis shows that some microRNAs downregulate large numbers of target mRNAs. *Nature* **433**, 769–773 (2005).

Supplementary Information is linked to the online version of the paper at www.nature.com/nature.

Author Contributions J.G.R. performed the computational analysis. C.H.J. performed the experimental analysis. All authors contributed to the design of the study and preparation of the manuscript.

Author Information Small RNA sequences were deposited in the Gene Expression Omnibus (www.ncbi.nlm.nih.gov/geo/), accessions GPL5061 and GSE7448. Reprints and permissions information is available at www.nature.com/reprints. The authors declare no competing financial interests. Correspondence and requests for materials should be addressed to D.P.B. (dbartel@wi.mit.edu).

METHODS

Computational methods. *D. melanogaster* small RNAs were from 2,075,098 high-throughput pyrosequencing reads[4] and are available at the GEO. *C. elegans* small RNA sequences were from ref. 5. Introns were defined according to FlyBase v4.2 *D. melanogaster* gene annotations[19]. *C. elegans* introns were defined using annotations and genomic sequence from WormBase (release WS120)[20]. *Mus musculus* introns were defined using NCBI RefSeq annotations[21] applied to the March 2005 release of the mouse genome available through UCSC (mm6)[22]. RNA secondary structures were predicted using RNAfold[26]. *D. melanogaster* intron conservation was assessed based on a nine-species multiZ alignment[25] of *D. melanogaster*, *Drosophila simulans*, *Drosophila yakuba*, *Drosophila ananassae*, *D. pseudoobscura*, *Drosophila virilis*, *Drosophila mojavensis*, *Anopheles gambiae* and *Apis mellifera* genomes, generated at UCSC[22]. Percentage nucleotide identity between *D. melanogaster* and *D. pseudoobscura* introns was calculated as the number of identity matches between the two orthologous introns in the multiZ alignment divided by the length of the longer intron. Introns not aligned between those two species were not tallied. *C. elegans* intron conservation was similarly determined using multiZ alignment of the *C. elegans* and *C. briggsae* (WormBase cb25.agp8)[20] genomes generated at UCSC[22]. Pre-miRNA lengths were calculated using miRBase v9.1 hairpin annotations[17]. Secondary structures were generated using RNAfold[26], and the miRNA* position was inferred on the basis of the annotated miRNA, assuming 2-nt 3′ overhangs. Pre-miRNA lengths were the sum of the miRNA length, the miRNA* length, and the length of intervening sequence.

Plasmids. Minigenes containing *mir-1003* and *mir-1006* and flanking exons were PCR amplified from genomic DNA. Minigenes for *mir-1006* and *mir-1003* were cloned into pMT-puro with the indicated sites to make expression plasmids pCJ19 and pCJ20, respectively. *let-7* was amplified from genomic DNA with primers 474 bp upstream and 310 bp downstream of the *let-7* hairpin and cloned into pMT-puro to make pCJ24. Similar minigenes replaced EGFP in p2032 (ref. 27) to give pCJ31 (*mir-1006*), pCJ30 (*mir-1003*) or pCJ32 (*let-7*). U1a snRNA and U1a-3G snRNA expression constructs were constructed essentially as described[13]. Sequences of inserts in pCJ19 (pMT-puro-*mir-1006*), pCJ20 (pMT-puro-*mir-1003*), pCJ24 (pMT-puro-*let-7*), pCJ30 (p2032-*mir-1003*), pCJ31 (p2032-*mir-1006*), and pCJ32 (p2032-*let-7*) are provided (Supplementary Table S4). Quikchange site-directed mutagenesis (Stratagene) was used to make 3′ splice site mutations with the indicated primers: *mir-1003* 3′ mut (CCTCTCACAT-TTACATATTCACGACGCCGTGAGCTGC and GCAGCTCACGGCGTCGT-GAATATGTAAATGTGAGAGG), and *mir-1006* 3′ mut (GGTACAATTTAAA-TTCGATTTCTTATTCATGCGTGCAATACCAGTTGATC and GATCAACT-GGTATTGCACGCATGAATAAGAAATCGAATTTAAATTGTACC). Similarly, *mir-1003* 5′ mut was made with the following mutagenic primers: (GCTGC-GCAGAACGTGGGCATCTGGATGTGGTTGGC and GCCAACCACATCCAG-ATGCCCACGTTCTGCGCAGC; CCTCTCACATTTACATGTTCACAGGCGC-CGTGAG and CTCACGGCGCCTGTGAACATGTAAATGTGAGAGG).

Luciferase-reporter inserts were made by annealing oligonucleotides with their reverse complements, leaving overhangs for the indicated restriction sites (lower case): let-7-ps (gagctcACTATACAACCTACTACCTCAaactagt), let-7-psm (gagctcACTATACAACCTACAAGCACAaactagt), miR-1003-ps (gagctcCT-GTGAATATGTAAATGTGAGAaactagt), miR-1003-psm (gagctcCTGTGAATA-TGTAAAAGAGTGAactagt), miR-1006-ps (gagctcCTATGAATAAGAAATCG-AATTTAactagt), and miR-1006-psm (gagctcCTATGAATAAGAAATCCAT-TATAactagt). Annealed oligos were ligated into *SacI*/*SpeI*-cleaved pIS2 (ref. 30). These plasmids were linearized with *Hind*III, polished with Klenow enzyme to create blunt ends, and digested with *Not*I to excise the *Renilla* luciferase gene with the modified UTR from the remainder of pIS2. The gel-purified *Renilla* gene fragment was then ligated into pMT-puro between *Eco*RV and *Not*I sites for copper-induced expression in S2 cells.

Cell culture and RNAi. S2-SFM cells were adapted from S2 cells to grow in *Drosophila* serum free media (SFM) by passaging into increasing amounts of SFM (0%, 25%, 50%, 75%, 90%, 100%), then grown in SFM supplemented with 2 mM L-glutamine at 25 °C in a humidified incubator. 5 μg of pCJ19 or pCJ20 were transfected into a 60 mm plate containing 2.5×10^6 S2 cells with FuGENE HD. Cells were grown for 3 days, split 1:10, and selected for 3 weeks in 10 μg ml^{-1} puromycin before experimentation, then maintained in 5 μg ml^{-1} puromycin.

Templates for dsRNA were amplified by PCR and extended to have convergent T7 promoters. 400 μl PCR reactions were phenol/chloroform extracted, ethanol precipitated, and used as template for 400 μl T7 transcriptions. Transcription reactions were treated with 20 U of DNase I for 15 min. The transcription products were then extracted in phenol:chloroform (5:1 pH 5.3) and ethanol precipitated. RNA was resuspended, desalted over Sephadex G-300, then heated to 75 °C for 10 min and slow cooled to room temperature. Yield and quality were assessed by agarose gel and UV absorbance. The sense sequence of each dsRNA is listed (Supplementary Table S4).

S2 cells were soaked in 10 μg ml^{-1} dsRNA in SFM. 500,000 cells were plated per well of a 24-well plate and soaked for 2 days, split 1:4, soaked another 2 days, expanded into 6-well plates, then soaked for three days. MicroRNA expression was induced by addition of 500 μM CuSO$_4$ to the growth media, and RNA harvested 12 h later with TRI reagent.

Northern blots were performed as described[5], using the following oligonucleotides (purchased from IDT) as probes for the indicated RNA species ('+' precedes LNA bases): ACTATACAACCTACTACCTCA (*let-7*), C+TGT+GAA+TAT+GTA+AAT+GTG+AGA (*mir-1003* probe 1), CCAACCACA-TCCAGATACCCACC (*mir-1003* probe 2), C+TAT+GAA+TAA+GAA+ATC+GAA+TTT+A (*mir-1006* probe 1), TTTACGCATTTCAATTTCAAA-CTCAC (*mir-1006* probe 2), TTGCGTGTCATCCTTGCGCAGG (U6).

RT–PCR. 500 ng mirtron plasmids were cotransfected with 500 ng either U1 or GFP carrier plasmid using 3 μl FuGENE HD per well of a 12 well plate. 24 h post-transfection, mirtron expression was induced for 36 h in the presence of 500 μM CuSO$_4$. Total RNA was extracted with TRI reagent, and 4 μg were treated with DNase using the DNA-free kit (Ambion). 500 ng DNA-free RNA were reverse-transcribed with oligo-dT(16) and Superscript III (Invitrogen) per manufacturers instructions. 1 μl cDNA was used as a template for PCR using exonic primers (ATAAAGCCGATAAGCGTGCG and CGTCCTTGTGCGTCTCC-TCC) flanking *mir-1003*. After 24 cycles of PCR, 10 μl of the reaction was resolved on an ethidium-stained 1.5% agarose gel and visualized by UV illumination.

Quantitative RT–PCR was performed on an ABI 7000 Real-Time PCR system with ABI Power SYBR Green reagents. First-strand synthesis was performed as above. The following primer pairs were used to amplify the specified mRNA: *actin 5c* (CCCATCTACGAGGGTTATGC, TTGATGTCACGGACGATTTC); *drosha* (TCACCATCCACGAGCTAGAC, ACGAAACGCGGAAAGAAGTG); *dicer-1* (GCCATTGAAGCATGACATTG, AAATCCCTCCTTGCCGATAG); *loquacious* (CGATTACCGAGTGGATACGG, CAAAGGAATCGGTGGAAAAG); *dicer-2* (GGCCACGAAACTTAAAGAGC, TGTGGAAAGGACACCATGAC); *r2d2* (GACGGAGGGTACGTCTGTAAA, AGCAGTTGGATTTTACGCAAG); *ldbr* (TTATCCCTGCCAGCACCTAC, CCTCTACATGAGGCGTTTCC).

Threshold cycle (Ct) and baseline were detected by ABI 7000 SDS software. *actin 5C* was used to calculate the ΔCt, and ΔΔCt was calculated by subtracting the ΔCt from that of the GFP dsRNA treated samples; the relative abundance was calculated as $1/(2^{\Delta\Delta Ct})$. Geometric mean ± standard deviation are shown for three replicate wells.

Luciferase assays. S2-SFM cells were plated 300,000 cells ml^{-1} in 96 well plates. After 24 h, cells were cotransfected with 96 ng microRNA-expressing plasmid, 4 ng perfect-site reporter and 2 ng firefly reporter per well using FuGENE HD (3 μl lipid per μg DNA). Expression of *Renilla* luciferase was induced 24 h post-transfection with 500 μM CuSO$_4$. Luciferase assays were performed 24 h post-induction with the Dual-Glo Luciferase system (Promega) on a Tecan Safire2 plate reader. The ratio of *Renilla*:firefly luciferase activity was measured for each well. To calculate fold repression, the ratio of *Renilla*:firefly for reporters with mutant sites was divided by the ratio of *Renilla*:firefly for reporters with wild-type sites. These values were also obtained in the presence of a plasmid expressing a non-cognate miRNA, and fold repression for the cognate miRNA was normalized to that of the non-cognate.